DOI: 10.54083/BRT/7.4.2025/112-117

Bio. Res. Today 2025, 7(4):112-117

Biotica Research Today

e-ISSN: 2582-6654

April, 2025

Article ID: RT1794 **Research Article**

Effect of Carbon Fiber Incorporation on Thermoelectric Performance of SnSe: An Environment Friendly Material for Waste Energy Harvesting

Kriti Tyagi[1,2*], Rohit Yadav[1,2], Harsh Yadav[3] and S.R. Dhakate[1,2]

[1]CSIR-National Physical Laboratory, Dr. K.S. Krishnan Marg, New Delhi (110 012), India

[2]Academy of Scientific & Innovative Research (AcSIR), Ghaziabad, Uttar Pradesh (201 002), India

[3]Dept. of Chemistry, Ramjas College, University of Delhi, New Delhi (110 007), India

Corresponding Author

Kriti Tyagi

: kriti.tyagi@nplindia.res.in

Conflict of interests: The author has declared that no conflict of interest exists.

How to cite this article?

Tyagi, K., Yadav, R., Yadav, H., *et al*., 2025. Effect of Carbon Fiber Incorporation on Thermoelectric Performance of SnSe: An Environment Friendly Material for Waste Energy Harvesting. *Biotica Research Today* 7(4), 112-117. DOI: 10.54083/BRT/7.4.2025/112-117.

Abstract

Thermoelectric (TE) materials, with their propensity to convert discarded waste heat into electrical energy, have attracted great interest as a source of renewable energy. In present work, we realized improvement in the thermoelectric behaviour of SnSe by composite formation with carbon fiber (CF). The CF incorporation into SnSe matrix leads to decoupling of the interdependent transport characteristics. The SnSe + x wt.% C.F. (x = 0, 0.2, 0.4, 0.6) composites have been prepared by spark plasma sintering process of the prepared composite powders. CF inclusion promotes transportation of charge carriers and contributes towards lower thermal conductivity ascribed to phonon scattering at the interface. A maximum zT value of around 1.1 was attained for SnSe + 0.2% CF at 773K. The contribution to improved zT originates from improved Seebeck coefficient and reduced thermal conductivity values. Our findings provide a probable approach to improve thermoelectric performance of SnSe.

Keywords: Carbon fiber, Figure-of-merit, Sustainability, Thermoelectrics

Introduction

There is a constantly increasing focus on green energy resources fueled by the never-ending demand for energy. As a repercussion of the globalization, non-renewable fossils fuels, are rendered incompetent of fulfilling the energy needs of the society (Yang *et al.*, 2025). In an effort to safeguard our environment, the focus has now shifted towards making society conscious of the quest for renewable energy sources. The majority of energy conversion/ production processes rely on thermal methods that result in generation of great amount of waste heat released into the environment (Lakshmanan and Upadhayay, 2024). Thermoelectric materials aid in promotion of sustainability by virtue of their potential to trasform rejected waste heat into electrical energy. This greatly helps in reduction of energy consumption and greenhouse gas emission (Osborne, 2022). The thermoelectric devices provide advantages over alternative conversion devices, namely, the absence of movable components, portability, low-maintenance, silent operation and scalability *etc*. (Wan *et al.*, 2015). Nevertheless, the low efficiency and increased cost of these materials limits their use. The thermoelectric devices have been employed in different space applications (Boccardi *et al.*, 2019; Janak *et al.*, 2015; Kilinc *et al.*, 2024), utilizing waste heat from human body to power smart watch (Mohammed *et al.*, 2021), in woodstoves for attainment of electricity from produced heat (Goudarzi *et al.*, 2013; Sornek, 2021), among various other applications (Martin-Gonzalez *et al.*, 2013).

The majority of commercialized thermoelectric devices are made up of Bismuth and Tellurium (Hatzikraniotis *et al.*, 2010), both of which falls in the category of rare earth elements and are known to be less abundantly available. Their use leads to increase in cost of manufacturing. The other class of thermoelectric materials with high efficiency comprise of moderately or highly toxic elements such as, Pb. Thus, in an attempt to engineer TEGs with safe and extensive applications, TE materials comprising richly available and non-toxic elemental constituents needs to be explored.

Article History

RECEIVED on 28th October 2024 RECEIVED in revised form 01st April 2025 ACCEPTED in final form 08th April 2025

The thermoelectrics research revolves around enhancing the figure-of-merit zT of the material, which directly measure its energy conversion efficiency. The figure-of-merit is assessed as: $zT = S^2\sigma T/\kappa$, where S, σ, T and κ indicates Seebeck coefficient, electrical conductivity, absolute temperature and thermal conductivity, respectively. Owing to the correlation among all these parameters, research have been expanded to unfolding new methods and concepts that would result in realization of improved thermoelectric performance (Faleev and Leonard, 2008; Heremans *et al.*, 2012; Pei *et al.*, 2011; He *et al.*, 2024). Tin Selenide (SnSe), having ultra-low thermal conductivity, is categorized as one of the most potential substances for medium temperature applications (Zhao *et al.*, 2016). A high zT value of 2.60 at 923K has been reported for SnSe single-crystal (Zhao *et al.*, 2014). However, inadequate mechanical strength of SnSe single crystals restricts their commercial applications.

An alternative strategy of composite formation of SnSe with carbon composite materials is considered to be promising approach for enhancing the thermoelectric as well as mechanical performance. For example, research showed that SnSe/CNT composites exhibited improvement in both Seebeck coefficient, electrical conductivity and suppression of lattice thermal conductivity, leading to ~90% increase in ZT for SnSe/CNT composite sample (Liu *et al.*, 2022). Researchers reported enhanced electronic transport properties by introduction of graphene nanoplatelets (GNPs) into SnSe matrix (Alsalama *et al.*, 2022). In another study (Li *et al.*, 2016), approximately 69% increase in power factor was reported due to electrical conductivity enhancement on introduction of 2.5% carbon black nanoinclusions in SnSe matrix. Similarly (Ju and Kim, 2016), inclusion of 1 wt.% SiC in SnSe framework improved ZT value owing to the production of interfaces within SnSe matrix that help to decline the thermal conductivity with simultaneous improving the Seebeck coefficient. In the past, carbon derivates have been incorporated into several thermoelectric matrices, however, various challenges impacted the potential of these derivatives in enhancing thermoelectric properties. The main challenge being the agglomeration issue of majority of carbon derivatives like graphene, CNTs *etc*. that led to non-uniform dispersion, in addition to, weak interface bonding (Ahmad *et al.*, 2019; Liang *et al.*, 2018; Ponraj *et al.*, 2017), thus, restricting their functionality towards boosting the thermoelectric performance of the composite.

Carbon Fiber (CF), with numerous advantages serves as potential additive composite material in thermoelectrics field attributable to exemplary thermal, electrical and mechanical properties (Bhatt and Goe, 2017). This research examines an effective method to boost the thermoelectric performance of SnSe material through the incorporation of carbon fiber (CF) in material matrix. Addition of CF into SnSe matrix aids in decoupling of interdependent thermoelectric parameters. Firstly, CF incorporation can enhance electrical conductivity due to increase in carrier concentration. Secondly, it helps in Seebeck coefficient value increment as a consequence of creation of interfaces that have the ability to filter low energy charge carriers. Lastly, these high-density interfaces aid in phonon scattering leading to suppression of thermal conductivity. In this research, we have examined the consequence of CF incorporation on thermoelectric performance of SnSe matrix. Results showed that CF incorporation led to enhancement in PF with simultaneous reduction in thermal conductivity. A reduced lattice thermal conductivity achieved (~0.36 W mK^{-1} at 773K) for SnSe + 0.2% CF results in a peak ZT of 1.1 at 773K.

Materials and Methods

SnSe samples were synthesized by weighing high purity elemental Sn and Se shots in appropriate ratio, vacuum-sealed in a quartz tube and annealed at 1273K for 24 hours. The SnSe ingot thus obtained was crushed into powder form. 5-6 µm diameter carbon fibers were minced as primary step towards composite formation. The carbon fibers weighed in different weight percentages according to the composition were ultrasonicated in ethanol medium. Towards the completion of ultrasonication time of 1 hr 30 min, the prepared SnSe powder is added to the ethanol and carbon fiber mixture. The solution is then immediately transferred to a hot plate stirrer and monitored on the stirrer until the ethanol evaporates to leave behind a thick slurry consisting of homogeneously dispersed carbon fiber and SnSe. The resultant slurry is oven dried for 5 hrs after which a dry hybrid SnSe-CF powder is obtained. To ensure homogeneous mixing of SnSe and CF, the SnSe-CF powder is grinded for 1 hr. The synthesis route followed is similar to the one adopted by Liang *et al.* (2019), for the formation of ZnO/carbon nanocomposites. The SnSe-CF powder were subsequently sintered using the spark plasma sintering technique (SPS) at 50 MPa pressure and temperature ~773K for 5 minutes, using 12.7 mm graphite die and punches. The sintered SnSe-CF composite pellets were glistened and cut into disc shaped specimens having thickness ~1.3 mm and diameter ~12.7 mm for thermal diffusivity measurements using Linseis Laser Flash analysis system (LFA1023). Electrical transport measurements (Seebeck coefficient and electrical conductivity) were carried out on rectangular bars ~10 mm in length and cross-section 3 mm × 3 mm under helium atmosphere (ULVAC ZEM-3). All transport property measurements were taken in a direction parallel to the pressing direction during SPS treatment. The samples were nomenclatured as SnSe, SnSe + 0.2% CF, SnSe + 0.4% CF, SnSe + 0.6% CF as per the weight percentage of CF in each sample. The structural investigation of the As-synthesized SnSe-CF composites was accomplished using powder X-ray diffraction (Rigaku 40 kV, 30 mA) instrument. Cu-Kα radiation was used as the source with 2θ in the range 20° to 80° and a step width of 0.02. Scanning Electron Microscopy (SEM, Zeiss Supra 40VP) was used to observe the elemental distribution of the As-synthesized SnSe-CF composites. The specific heat capacity of the sample was reckoned through Differential Scanning Calorimeter (Netzsch, DSC 404F3). Conventional Archimedes principle was employed to determine the density of the synthesized pellets and was found to be ~99% of the theoretically observed density for all the synthesized samples. The accuracies in measurements are: ±0.5% for density, ±5% for specific heat, ±7% for electronic transport

measurements, ±6% for thermal diffusivity.

Results and Discussion

Microstructural Characterization

The X-ray diffraction characteristics of pristine and x% CF incorporated SnSe composite samples are depicted in figure 1. The data reveals the single phase of SnSe for all the samples having low symmetry orthorhombic phase. The absence of a secondary phase like carbon, within the detection limit, indicates no changes in SnSe structure upon carbon fiber addition. The samples are preferably oriented perpendicular to the pressing direction and exhibit the strongest peak at 400.

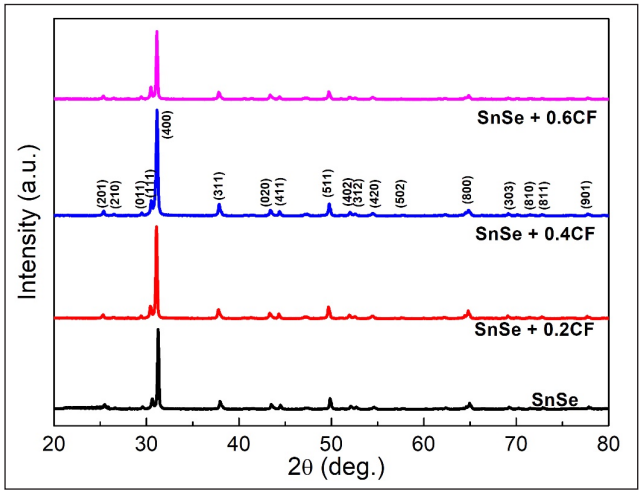

Figure 1: X-ray analysis patterns of SnSe + x% CF (x = 0 - 0.6)

The microstructural investigation was accomplished to examine the morphology along with the distribution of CF in the SnSe-CF samples. The SEM depictions in backscattered diffraction mode for SnSe + 0.2% CF, SnSe + 0.4% CF and SnSe + 0.6% CF composites are depicted in figure 2. From the images, we observe uniform grain size distribution throughout SnSe matrix with CF (black spots) dispersed uniformly within the entire matrix. From the magnified images shown in insets, it is visible that the fibers have a length ranging from few mm to ~50 mm.

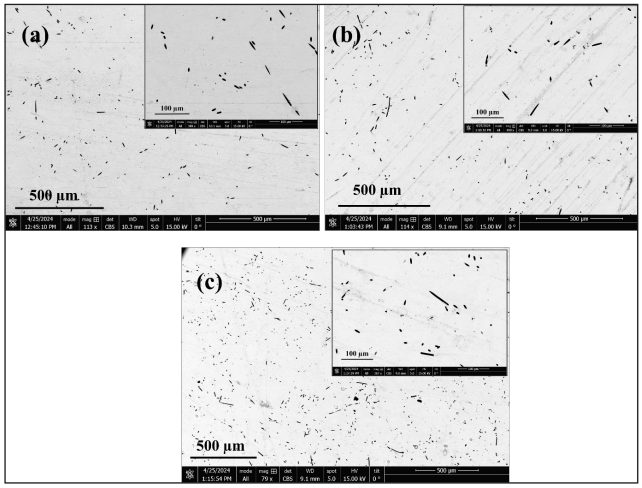

Figure 2: EBSD images of the As-synthesized (a) SnSe + 0.2% CF, (b) SnSe + 0.4% CF, (c) SnSe + 0.6% CF

Figure 3 exhibits the FESEM image of the broken surface of pure SnSe. An apparent layered structure is visible for the pure compound (Figure 3a). Figure 3(b) and 3(c) displays the FESEM image of fractured surface of SnSe + 0.2% CF pellet after SPS. It can be observed that the diameter of the CF in SnSe-CF composite was about 4-5 µm. The elemental distribution maps for an exposed fiber in the SnSe matrix is shown in figure 3(d). The EDS mapping shows that some Sn content was absorbed selectively on to the CF surface (Figure 3e).

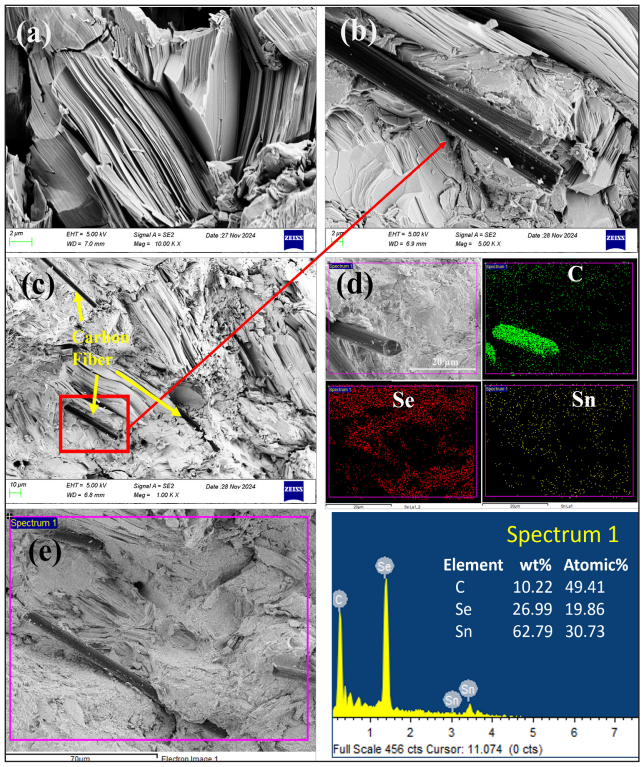

Figure 3: SEM micrograph depiction and elemental maps of As-synthesized SnSe and SnSe-CF composites: (a) SEM image of the broken surface of pristine SnSe; (b) and (c) secondary electron image of the fractured facet of SnSe + 0.2% CF at different magnification; (d) EDS mapping of SnSe + 0.2% CF, focusing on the exposed fiber; and (e) Elemental composition of SnSe-CF sample as obtained employing EDS

Transport Properties

Figure 4 shows the electronic transport characteristics of As-synthesized samples SnSe + x wt.% CF (x = 0 - 0.6) w.r.t. temperature. The measurements are conducted in a direction orthogonal to the pressing direction during SPS treatment. The electrical conductivity (σ) of undoped SnSe [Figure 4(a)] is lowest at the room temperature (73.8 S m^{-1}). After composite formation with CF, the σ value is enhanced to 772 S m^{-1} and 560 S m^{-1} for 0.4% and 0.6% CF, respectively. The σ values for all the samples rapidly increase beyond 600K, exhibiting semiconducting behavior. Similar behavior has also been reported earlier by different research groups (Chen *et al.*, 2014; Leng *et al.*, 2016; Yang *et al.*, 2017). No significant improvement in σ at room temperature and in entire temperature range was observed for 0.2% CF introduction, indicating that 0.2% CF

sample does not contribute towards σ and is not sufficient to qualify as electron acceptor to induce shift in the Fermi level. Interestingly, for the greater concentration values of 0.4% and 0.6% CF, σ records a significant increase at room temperature, with considerably high value of σ for 0.6% CF at 773K.

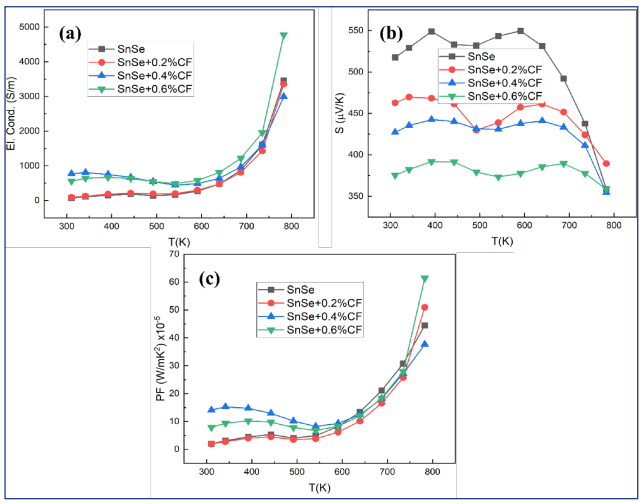

Figure 4: Temperature reliance of electrical characteristics of SnSe + x% CF (x = 0 - 0.6): (a) Electrical Conductivity (σ), (b) Seebeck coefficient (S) and (c) power factor ($S^2\sigma$)

Figure 4(b) depicts the temperature reliant behavior of Seebeck coefficient (*S*) for SnSe + x% CF samples. In case of pristine SnSe, the value for *S* is ~517 μV K^{-1} at 300K which decreases to 358 μV K^{-1} at 773K. With increasing concentrations of CF, *S* value decreases appreciably owing to enhancement in carrier concentration. The highest recorded value of S at operating temperature 773 K is observed for SnSe + 0.2% CF (390 μV K^{-1}). Also, the trend of graphs confirms transformation of samples from *Pnma* lower symmetry SnSe phase to *Cmcm* high symmetry SnSe phase. Due to the outstanding electrical conductivity values and appreciable Seebeck coefficient, SnSe + x% CF samples showcases enhanced power factor (PF) S^2s, as depicted in figure 4(c). The PF value for undoped SnSe at 773K is reported to be 444 μW mK^{-2}, while maximum PF value of 614 μW mK^{-2} at same temperature is obtained for SnSe + 0.6% CF sample. This value of PF for SnSe + 0.6% CF sample is higher in comparison to the value noted by Yang *et al.* (2020) for SnSe-CF samples (388 μW mK^{-2} at 823K).

The fluctuation of total thermal conductivity (κ) on temperature for SnSe + x% CF is illustrated in figure 5(a). The lowest κ at 773K is observed for SnSe + 0.2% CF sample (0.36 W mK^{-1}). The additional scattering at the grain boundaries introduced as an outcome of CF addition leads to decrease in κ values.

Figure 5(b) shows fluctuation of ZT in the entire temperature range for SnSe + x% CF samples. The ZT value of SnSe + 0.4% CF is significantly higher upto 623K as compared to other samples and attains a maxima of 0.79 at 773K. However, the maximal value of ZT at operating temperature is recorded for SnSe + 0.2% CF (1.1 at 773K), owing to significant power-factor and lowest value of κ at this temperature.

Vicker's Micro-Hardness Studies

Micro-hardness studies aid in evaluation of material's mechanical strength. It is a well-known fact that the thermoelectric research has been directed towards enhancement of electronic and thermal transport properties of the material. However, the mechanical properties also play an crucial role in accessing long term solidity of the thermoelectric modules. With the help of micro-hardness analysis, we can access the mechanical characteristics of the material. Here, SnSe + x% CF samples were analysed using Vicker's micro-hardness tester that determines the hardness of the material using the equation:

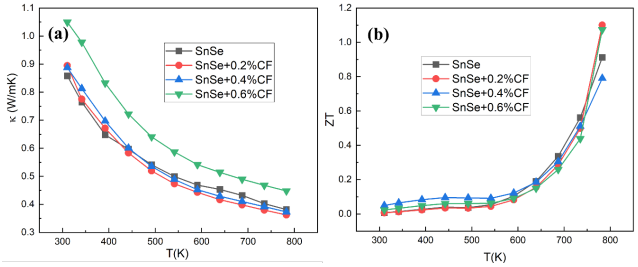

Figure 5: Temperature variation of: (a) thermal conductivity and (b) figure-of-merit ZT of SnSe + x% CF (x = 0 - 0.6) samples

$H_v = 1.854\ (P/d^2)$ ..... (1)

Where, H_v corresponds to Vicker's hardness number, the entity P represents applied load and *d* stands for average length of indentation imprint when measured diagonally. SnSe is a layered compound and thus, showcases poor mechanical properties. CF acts as reinforcing agent, thus, providing additional strength to the composite.

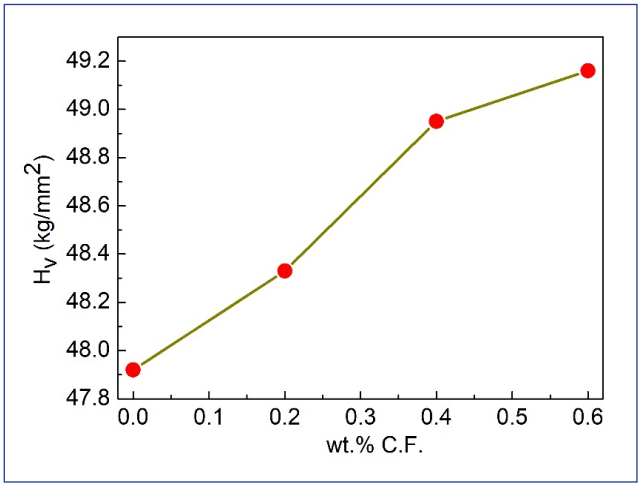

Figure 6: Variation of hardness number H_v with carbon fiber content for SnSe + x% CF (x = 0 - 0.6) samples

It is observed that, on application of 100 g load, hardness number (H_v) rises with increase in carbon fiber content in SnSe matrix, as shown in figure 6. The increase in hardness number for SnSe-CF composites hints towards the fact that the high value of Young's Modulus for CF (250 GPa (Yang *et al.*, 2020)) as compared to SnSe (65 GPa (Tyagi *et al.*, 2016)), renders the CF network inside the SnSe matrix capable of bearing the applied load in an attempt to resist deformation.

Also, enhancement in mechanical properties by integration of carbon in material matrix has been reported in different thermoelectric class of materials (Anjum *et al.*, 2024; Jia *et al.*, 2024; Ojha *et al.*, 2024).

Conclusion

Composite formation with carbon fiber successfully leads to enhancement in thermoelectric properties of SnSe. A maximal power factor of 614 μW mK^{-2} at 773K was realized for SnSe + 0.6% CF sample. On account of the grain boundary scattering owing to carbon fiber introduction, the κ was reduced to 0.36 W mK^{-1} at 773K, yielding highest ZT of 1.1 at 773K for SnSe + 0.2 wt.% carbon fiber sample. These research findings suggest that the introduction of carbon fiber into SnSe matrix qualifies as favourable strategy towards enhancement of the thermoelectric performance. Composite approach using carbon fiber incorporation in SnSe matrix opens up new avenue for improvement of thermoelectric performance in other class of materials.

Acknowledgements

Authors thank the Science and Engineering Research Board (SERB) for SIRE fellowship grant (SIR/2022/000958), Indo-German Technology Centre for the WISER Grant (IGSTC/WISER2023/KT/34/2023-24) and CSIR-National Physical Laboratory for research facilities. Authors are also pleased to CSIR, India, for financial support through the CSIR Junior Research Fellowship (JRF) and to AcSIR-NPL, India, for Ph.D. registration.

References

Ahmad, K., Wan, C., Al-Eshaikh, M.A., Kadachi, A.N., 2019. Enhanced thermoelectric performance of Bi_2Te_3 based graphene nanocomposites. *Applied Surface Science* 474, 2-8. DOI: https://doi.org/10.1016/j.apsusc.2018.10.163.

Alsalama, M., Hamoudi, H., Abdala, A., Youssef, K.M., 2022. Effect of graphene on thermal stability of tin selenide. *Journal of Materials Research and Technology* 18, 896-908. DOI: https://doi.org/10.1016/j.jmrt.2022.02.045.

Anjum, F., Dixit, P., Maiti, T., 2024. Enhanced thermoelectric performance with improved mechanical strength in Bi_2S_3/graphite composites. *Carbon* 218, 118692. DOI: https://doi.org/10.1016/j.carbon.2023.118692.

Bhatt, P., Goe, A., 2017. Carbon fibres: Production, properties and potential use. *Material Science Research India* 14(1), 52-57. DOI: http://dx.doi.org/10.13005/msri/140109.

Boccardi, S., Ciampa, F., Meo, M., 2019. Design and development of a heatsink for thermo-electric power harvesting in aerospace applications. *Smart Materials and Structures* 28(10), 105057. DOI: https://doi.org/10.1088/1361-665X/aacbac.

Chen, C.L., Wang, H., Chen, Y.Y., Day, T., Snyder, G.J., 2014. Thermoelectric properties of p-type polycrystalline SnSe doped with Ag. *Journal of Materials Chemistry A* 2(29), 11171-11176. DOI: https://doi.org/10.1039/C4TA01643B.

Faleev, S.V., Leonard, F., 2008. Theory of enhancement of thermoelectric properties of materials with nanoinclusions. *Physical Review B: Condensed Matter and Materials Physics* 77(21), 214304. DOI: https://doi.org/10.1103/PhysRevB.77.214304.

Goudarzi, A.M., Mazandarani, P., Panahi, R., Behsaz, H., Rezania, A., Rosendahl, L.A., 2013. Integration of thermoelectric generators and wood stove to produce heat, hot water and electrical power. *Journal of Electronic Materials* 42, 2127-2133. DOI: https://doi.org/10.1007/s11664-013-2545-8.

Hatzikraniotis, E., Zorbas, K.T., Samaras, I., Kyratsi, Th., Paraskevopoulos, K.M., 2010. Efficiency study of a commercial thermoelectric power generator (TEG) under thermal cycling. *Journal of Electronic Materials* 39, 2112-2116. DOI: https://doi.org/10.1007/s11664-009-0988-8.

He, Q., Yang, D., Xia, S., Song, H., 2024. Ultra-low thermal conductivity and improved thermoelectric performance in La_2O_3-dispersed $Bi_2Sr_2Co_2O_y$ ceramics. *Materials Science and Engineering: B* 299, 116976. DOI: https://doi.org/10.1016/j.mseb.2023.116976.

Heremans, J.P., Wiendlocha, B., Chamoire, A.M., 2012. Resonant levels in bulk thermoelectric semiconductors. *Energy & Environmental Science* 5, 5510-5530. DOI: https://doi.org/10.1039/C1EE02612G.

Janak, L., Ancik, Z., Vetiska, J., Hadas, Z., 2015. Thermoelectric generator based on MEMS module as an electric power backup in aerospace applicat ions. *Materials Today: Proceedings* 2(2), 865. DOI: https://doi.org/10.1016/j.matpr.2015.05.112.

Jia, S., Qian, W., Yu, P., Li, K., Li, M., Lan, J., Lin, Y.H., Yang, X., 2024. Ionic thermoelectric materials: Innovations and challenges. *Materials Today Physics* 42, 101375. DOI: https://doi.org/10.1016/j.mtphys.2024.101375.

Ju, H., Kim, J., 2016. Effect of SiC ceramics on thermoelectric properties of SiC/SnSe composites for solid-state thermoelectric applications. *Ceramics International* 42, 9550. DOI: https://doi.org/10.1016/j.ceramint.2016.03.035.

Kilinc, E., Uysal, F., Sari, M.A., Kurt, H., Celik, E., 2024. Production of ZnAlO semiconducting materials for thermoelectric generators in potential aerospace applications. *Journal of Materials Science: Materials in Electronics* 35, 1835. DOI: https://doi.org/10.1007/s10854-024-13601-5.

Lakshmanan, S., Upadhayay, A., 2024. Vehicular emission scenarios in selected regions of India as per vehicular emission norms. *Research Biotica* 6(2), 87-94. DOI: https://doi.org/10.54083/ResBio/6.2.2024/87-94.

Leng, H., Zhou, M., Zhao, J., Han, Y., Li, L., 2016. Optimization of thermoelectric performance of anisotropic $Ag_xSn_{1-x}Se$ compounds. *Journal of Electronic Materials* 45, 527-534. DOI: https://doi.org/10.1007/s11664-015-4143-4.

Li, J.C., Li, D., Xu, W., Qin, X.Y., Li, Y.Y., Zhang, J., 2016. Enhanced thermoelectric performance of SnSe based composites with carbon black nanoinclusions. *Applied Physics Letters* 109, 173902. DOI: http://dx.doi.org/10.1063/1.4966126.

Liang, A., Jiang, X., Hong, X., Jiang, Y., Shao, Z., Zhu, D., 2018. Recent developments concerning the dispersion methods and mechanisms of graphene. *Coatings* 8(1), 33. DOI: https://doi.org/10.3390/coatings8010033.

Liang, X., Yang, Y., Dai, F., Wang, C., 2019. Orientation dependent physical transport behavior and the micro-mechanical response of ZnO nanocomposites induced by SWCNTs and graphene: Importance of intrinsic anisotropy and interfaces. *Journal of Materials Chemistry C* 7, 1208-1221. DOI: https://doi.org/10.1039/C8TC05148H.

Liu, X., Wang, H., Chen, Y., Zhang, B., Zhang, H., Zheng, S., Chen, X., Lu, X., Wang, G., Zhou, X., Han, G., 2022. Simultaneously optimized thermoelectric and mechanical performance of p-type polycrystalline SnSe enabled by CNTs addition. *Scripta Materialia* 218, 114846. DOI: https://doi.org/10.1016/j.scriptamat.2022.114846.

Martin-Gonzalez, M., Caballero-Calero, O., Diaz-Chao, P., 2013. Nanoengineering thermoelectrics for 21st century: Energy harvesting and other trends in the field. *Renewable and Sustainable Energy Reviews* 24, 288-305. DOI: https://doi.org/10.1016/j.rser.2013.03.008.

Mohammed, N., Wang, R., Jackson, R.W., Noh, Y., Gummeson, J., Lee, S.I., 2021. ShaZam: Charge-free wearable devices *via* intra-body power transfer from everyday objects. *Proceedings of the ACM on Interactive, Mobile, Wearable and Ubiquitous Technologies* 5(2), 1-25. DOI: https://doi.org/10.1145/3463505.

Ojha, A., Nanda, U., Pradhan, A., Bathula, S., 2024. Enhancement of mechanical performance and reduction in thermal conductivity of Mg_2Si-based thermoelectric nanocomposites through rGO addition. *Applied Physics A* 130(12), 905. DOI: https://doi.org/10.1007/s00339-024-08061-x.

Osborne, R., 2022. Join the fight against fossil fuels. *British Medical Journal* 379, o2414. DOI: https://doi.org/10.1136/bmj.o2414.

Pei, Y., Shi, X., LaLonde, A., Wang, H., Chen, L., Snyder, G.J., 2011. Convergence of electronic bands for high performance bulk thermoelectrics. *Nature* 473, 66-69. DOI: https://doi.org/10.1038/nature09996.

Ponraj, N.V., Vettivel, S.C., Azhagurajan, A., Shajan, X.S., Nabhiraj, P.Y., Theivasanthi, T., Selvakumar, P., Lenin, A.H., 2017. Effect of milling on dispersion of graphene nanosheet reinforcement in different morphology copper powder matrix. *Surfaces and Interfaces* 9, 260-265. DOI: https://doi.org/10.1016/j.surfin.2017.10.006.

Sornek, K., 2021. Study of operation of the thermoelectric generators dedicated to wood-fired stoves. *Energies* 14(19), 6264. DOI: https://doi.org/10.3390/en14196264.

Tyagi, K., Gahtori, B., Bathula, S., Singh, N.K., Bishnoi, S., Auluck, S., Srivastava, A.K., Dhar, A., 2016. Electrical transport and mechanical properties of thermoelectric tin selenide. *RSC Advances* 6, 11562-11569. DOI: https://doi.org/10.1039/C5RA23742D.

Wan, C., Gu, X., Dang, F., Itoh, T., Wang, Y., Sasaki, H., Kondo, M., Koga, K., Yabuki, K., Snyder, G.J., Yang, R., Koumoto, K., 2015. Flexible n-type thermoelectric materials by organic intercalation of layered transition metal dichalcogenide TiS_2. *Nature Materials* 14, 622-627. DOI: https://doi.org/10.1038/NMAT4251.

Yang, S., Si, J., Su, Q., Wu, H., 2017. Enhanced thermoelectric performance of SnSe doped with layered MoS_2/graphene. *Materials Letters* 193, 146-149. DOI: https://doi.org/10.1016/j.matlet.2017.01.079.

Yang, G., Sang, L., Li, M., Islam, K.N., Yue, Z., Liu, L., Li, J., Mitchell, D.R.G., Ye, N., Wang, X., 2020. Enhancing the thermoelectric performance of polycrystalline SnSe by decoupling electrical and thermal transport through carbon fiber incorporation. *ACS Applied Materials & Interfaces* 12, 12910-12918. DOI: https://dx.doi.org/10.1021/acsami.0c00873.

Yang, X., Shi, T., Bao, W., Wang, Z., Wang, J., Wu, P., Zhang, Y., Feng, J., Ge, Z., 2025. Ultrahigh average zT realized in polycrystalline $SnSe_{0.95}$ materials through Sn stabilizing and carrier modulation. *Journal of Materiomics* 11(2), 100880. DOI: https://doi/org/10.1016/j.jmat.2024.04.006.

Zhao, L., Lo, S., Zhang, Y., Sun, H., Tan, G., Uher, C., Wolverton, C., Dravid, V.P., Kanatzidis, M.G., 2014. Ultralow thermal conductivity and high thermoelectric figure of merit in SnSe crystals. *Nature* 508, 373-377. DOI: https://doi.org/10.1038/nature13184.

Zhao, L., Chang, C., Tan, G., Kanatzidis, M.G., 2016. SnSe: A remarkable new thermoelectric material. *Energy & Environmental Science* 9, 3044-3060. DOI: https://doi.org/10.1039/C6EE01755J.